

# Dimensional crossover and the magnetic transition in electron doped manganites

Andrzej M. Oleś<sup>1,2</sup> and Giniyat Khaliullin<sup>1</sup>

<sup>1</sup>Max-Planck-Institut für Festkörperforschung, Heisenbergstrasse 1, D-70569 Stuttgart, Germany

<sup>2</sup>Marian Smoluchowski Institute of Physics, Jagellonian University, Reymonta 4, PL-30059 Kraków, Poland

(Dated: November 10, 2018)

We introduce a microscopic model for electron doped manganites that explains the mechanism of the observed transition from  $G$ -type antiferromagnetic ( $G$ -AF) to  $C$ -type antiferromagnetic ( $C$ -AF) order under increasing doping by double exchange mechanism. The model unravels the crucial role played by  $e_g$  orbital degrees of freedom and explains the observed metal-to-insulator transition by a dimensional crossover at the magnetic phase transition. The specific heat and the spin canting angle found for the  $G$ -AF phase agree with the experimental findings. As a surprising outcome of the theory we find that spin canting is suppressed in the  $C$ -AF phase, in agreement with the experiment, due to the Fermi surface topology.

Published in: *Phys. Rev. B* **84**, 214414 (2011).

PACS numbers: 75.25.Dk, 71.30.+h, 71.38.-k, 75.47.Gk

## I. INTRODUCTION

Doped transition metal compounds exhibit a number of very interesting and fascinating phenomena, including high temperature superconductivity in cuprates<sup>1</sup> or pnictides,<sup>2</sup> and colossal magnetoresistance in manganites.<sup>3</sup> The hole-doped perovskite manganites are well known for their complexity, originating from the competing tendencies in their rich phase diagrams,<sup>4</sup> with a variety of spin, charge and orbital orders. Several phases are energetically close to each other and small changes of electronic parameters or electron concentration result in phase transitions.<sup>3,5</sup> Hole doping, realized e.g. in  $\text{La}_{1-y}(\text{Ca,Sr})_y\text{MnO}_3$  for increasing  $y$ , triggers then a transition from an antiferromagnetic (AF) to a ferromagnetic (FM) phase by the double-exchange (DE) mechanism<sup>6</sup> that became a crucial idea to explain the onset of the metallic FM phase and electronic transport.

The DE model is one of the most widespread models of ferromagnetism. It describes the kinetic energy of electronic charge carriers coupled by Hund's exchange to localized  $t_{2g}$  spins interacting by AF superexchange. A pioneering work by de Gennes<sup>7</sup> suggested that the competition between FM DE interaction that arises in doped systems and AF superexchange between  $t_{2g}$  spins leads to spin-canted AF order. Extensive studies of these ideas led to progress in the theoretical understanding of the phase diagrams of hole doped manganites,<sup>3,5,8,9</sup> while electron doped systems were not analyzed carefully until now. In recent years the DE model was used to study, *inter alia*, striped multiferroic phases in doped manganites,<sup>10,11</sup> evolution of spin, orbital and charge order at interfaces,<sup>12</sup> valence fluctuations in magnetite,<sup>13</sup> novel spin phases on frustrated lattices,<sup>14</sup> and unusual spin superstructure observed in several vanadium spinels with degenerate  $t_{2g}$  orbitals.<sup>15</sup> In all these cases  $e_g$  orbital degeneracy plays a crucial role and might lead to anisotropic AF phases: either  $C$ -type AF ( $C$ -AF) or  $A$ -type AF ( $A$ -AF) phase,<sup>16</sup> depending on the electronic filling and the strength of AF superexchange.<sup>17</sup>

Usually, however, accurate studies of the DE model were hindered by the presence of strong intraorbital Coulomb interaction  $U$  in a lattice distorted by strong cooperative Jahn-Teller effect.<sup>5,18</sup> A qualitatively different situation arises in an ideal cubic perovskite  $\text{SrMnO}_3$ , with  $e_g$  bands being completely empty. Here the only interaction is AF superexchange between  $S = 3/2$  spins at  $\text{Mn}^{4+}$  ions. They are generated by  $t_{2g}$  charge excitations<sup>19</sup> and stabilize the isotropic three-dimensional (3D)  $G$ -type AF ( $G$ -AF) phase.<sup>16</sup> Weakly doped  $\text{SrMnO}_3$  represents an ideal situation for the DE model as the  $e_g$  electrons hardly interact with each other at low doping  $x$  and strong on-site Coulomb interactions between them may be neglected. In this case the DE model can be almost exactly solved under a single approximation, i.e., neglecting weak quantum fluctuations of large  $S = 3/2$  spins.

Early studies of electron doped  $\text{Ca}_{1-x/2}\text{Ce}_{x/2}\text{MnO}_3$  systems gave a magnetic transition to the  $C$ -AF phase.<sup>20</sup> The magnetic order in doped  $\text{CaMnO}_3$  was analyzed within the density-functional theory calculations that give instead a transition from the  $G$ -AF to  $A$ -AF phase.<sup>21</sup> Recently single crystals of  $\text{Sr}_{1-x}\text{La}_x\text{MnO}_3$  and  $\text{Sr}_{1-x/2}\text{Ce}_{x/2}\text{MnO}_3$  were synthesized and investigated,<sup>22</sup> showing that the transition to the  $C$ -AF phase occurs in both systems, in agreement with the prediction by Maezono *et al.*,<sup>8</sup> and the magnetic phase diagram is remarkably universal as a function of doping  $x$ .

In electron doped manganites chemical doping of  $\text{Sr}^{2+}$  with  $\text{La}^{3+}$  ( $\text{Ce}^{4+}$ ) ions generates  $e_g$  electronic carriers at  $\text{Mn}^{3+}$  ions. Following the standard picture of de Gennes,<sup>7</sup> one expects spin canting on AF bonds. Until recently only one exception from this rule was reported — spin canting is absent in the  $A$ -AF phase when electrons occupy  $x^2 - y^2$  orbitals and the hopping along AF bonds between FM  $ab$  planes is blocked.<sup>8</sup> In this context the recent experimental result of no canting in the  $C$ -AF phase<sup>22</sup> is puzzling and requires theoretical explanation, as hopping on the AF bonds in  $ab$  planes is there finite for electrons within  $3z^2 - r^2$  orbitals, and spin canting is expected.

Hole doped  $\text{La}_{1-y}\text{Sr}_y\text{MnO}_3$  manganites with large  $e_g$  electron density remain insulating up to  $y \simeq 0.17$ ,<sup>4</sup> as the metallic behavior is hindered here by formation of orbital polarons.<sup>23,24</sup> This is in sharp contrast with the electron doped systems with the  $G$ -AF *metallic* phase found in  $\text{Sr}_{1-x}\text{La}_x\text{MnO}_3$  by Sakai *et al.*<sup>22</sup> already at a very low electron doping  $x = 0.01$ . Surprisingly, when doping increases further to  $x \simeq 0.04$  this 3D weakly metallic phase changes to an insulating phase with quasi one-dimensional (1D) orbital order of partly occupied  $3z^2-r^2$  orbitals, accompanied by tetragonal lattice distortion and the  $C$ -AF spin order.

In this paper we investigate the DE model for doped  $e_g$  electrons, extended here by the coupling to the tetragonal lattice distortion which occurs in the  $C$ -AF phase. We derive the exact electronic structure, show a remarkable difference between the Fermi surface topology in the above magnetic phases, and demonstrate that it explains the absence of spin canting in the  $C$ -AF phase. The calculated values of the specific heat coefficient  $\gamma$  and the critical doping  $x_c$  for the  $G$ -AF/ $C$ -AF phase transition are in quantitative agreement with experiment.

The paper is organized as follows. In Sec. II we introduce the microscopic model and specify its parameters. The model is solved in Sec. III, where we analyze the remarkable difference between the electronic structure found in two magnetic phases. This leads to the magnetic transition which occurs under increasing doping as we show in Sec. IV. The paper is summarized in Sec. V.

## II. THE DOUBLE EXCHANGE MODEL

We consider the DE model for degenerate  $e_g$  electrons,<sup>17</sup> extended by the coupling to the lattice,

$$\mathcal{H} = - \sum_{ij,\alpha\beta,\sigma} t_{\alpha\beta}^{ij} c_{i\alpha\sigma}^\dagger c_{j\beta\sigma} - 2J_H \sum_i \vec{S}_i \cdot \vec{s}_i + J \sum_{\langle ij \rangle} \vec{S}_i \cdot \vec{S}_j - gu \sum_i (n_{iz} - n_{ix}) + \frac{1}{2} NKu^2. \quad (1)$$

Here the  $c_{i\alpha\sigma}^\dagger$  operator creates an electron with spin  $\sigma = \uparrow, \downarrow$  in orbital  $\alpha = z, x$  at site  $i$ , and  $n_{i\alpha} \equiv \sum_\sigma c_{i\alpha\sigma}^\dagger c_{j\alpha\sigma}$  in electron density in orbital state  $\alpha$  at site  $i$ , and  $N$  is the number of sites. Two  $e_g$  orbitals are labeled as

$$z \equiv (3z^2 - r^2)/\sqrt{6}, \quad x \equiv (x^2 - y^2)/\sqrt{2}, \quad (2)$$

and correspond to two components of the pseudospin  $\tau = 1/2$ . The hopping elements between a pair of nearest neighbors ( $ij$ ) along the axis  $\gamma = a, b, c$  are:

$$t_{\alpha\beta}^{a/b} = \frac{t}{4} \begin{pmatrix} 1 & \pm\sqrt{3} \\ \pm\sqrt{3} & 3 \end{pmatrix}, \quad t_{\alpha\beta}^c = t \begin{pmatrix} 1 & 0 \\ 0 & 0 \end{pmatrix}, \quad (3)$$

where  $t$  is an effective ( $dd\sigma$ ) hopping element between two  $3z^2-r^2$  orbitals along the  $c$  cubic axis. Following the

estimates of  $t$  performed within the polaronic picture<sup>23</sup> and using the optical spectroscopy for  $\text{LaMnO}_3$ ,<sup>25</sup> we fix the effective ( $dd\sigma$ ) hopping element at  $t = 0.4$  eV.

Hund's exchange between  $e_g$  and  $t_{2g}$  electrons at  $\text{Mn}^{4+}$  ions  $J_H \simeq 0.74$  eV is here the largest parameter. It aligns the spin of an  $e_g$  electron  $\vec{s}_i$  with the localized  $t_{2g}$  spin  $\vec{S}_i$  at site  $i$ . In this way the electronic structure depends crucially on the magnetic order of localized  $t_{2g}$  spins  $\{\vec{S}_i\}$  that interact by the nearest neighbor AF superexchange  $J > 0$ . It follows from virtual charge excitations  $d_i^3 d_j^3 \rightleftharpoons d_i^4 d_j^2$  along nearest-neighbor bonds  $\langle ij \rangle$  in the presence of strong on-site Coulomb interaction  $U$  between  $t_{2g}$  electrons.<sup>19</sup>

The tetragonal distortion  $u$  is finite only in the  $C$ -AF phase.<sup>22</sup> Here we define it as proportional to a difference between two lattice constants  $a$  and  $c$  along the respective axis,  $u \equiv 2(c - a)/(c + a)$ . Increasing lattice distortion ( $u > 0$ ) causes increasing  $e_g$  orbital splitting  $4E_{JT}$  determined by the Jahn-Teller energy,  $E_{JT} = g^2/2K \simeq 0.2$  eV.<sup>23</sup> Furthermore, using the experimental data of Ref. 22, we arrived at a semiempirical relation  $u \simeq 3x/20$ .

## III. ELECTRONIC STRUCTURE

Following de Gennes,<sup>7</sup> we determined the electronic structure for the  $G$ -AF phase by considering spin canting by angle  $\theta$  caused by electron doping. Hund's exchange at each site favors aligned  $t_{2g}$  and  $e_g$  electron spin states. To solve the electronic structure we introduce the fermion  $\{f_{i\alpha\sigma}^\dagger\}$  operators in a canted spin background using the local coordinate frame, for instance,

$$c_{i\alpha\uparrow}^\dagger = \cos(\theta/2) f_{i\alpha\uparrow}^\dagger - \sin(\theta/2) f_{i\alpha\downarrow}^\dagger. \quad (4)$$

The canting of each spin by angle  $\theta \in [0, \pi/2]$  (other states are equivalent) corresponds for  $\theta = 0$  ( $\pi/2$ ) to the AF (FM) spin order. The canting modulates the hopping elements between neighboring sites, and one finds an analytic solution for two (majority)  $e_g$  bands in the  $G$ -AF phase for spins being parallel to the  $t_{2g}$  spins at each site due to Hund's exchange,

$$\varepsilon_{\mathbf{k}}^\pm = -\sqrt{(t \sin \theta \gamma_{\mathbf{k}}^\pm + J_H S)^2 + (t \cos \theta \gamma_{\mathbf{k}}^\pm)^2}, \quad (5)$$

where

$$\gamma_{\mathbf{k}}^\pm = \sum_\lambda \cos k_\lambda \pm \left\{ \sum_\lambda \cos^2 k_\lambda - \cos k_x \cos k_y - \cos k_y \cos k_z - \cos k_z \cos k_x \right\}^{1/2}, \quad (6)$$

and the summations in Eq. (6) are over three cubic directions in momentum space, i.e.,  $\lambda = x, y, z$ . The remaining  $e_g$  bands correspond to excited states of  $e_g$  electrons with spins antiparallel to those of localized  $t_{2g}$  electrons

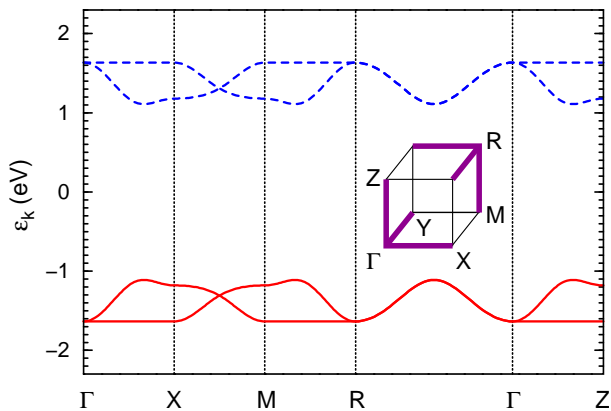


FIG. 1: (Color online) Band structure in the  $G$ -AF phase along the high symmetry directions. Spin majority (minority) bands are shown by solid (dashed) lines. Parameters:  $t = 0.4$  eV,  $J_H = 0.74$  eV,  $x = 0$ . Inset shows the Fermi surface at low doping (heavy lines along  $\Gamma - X$ ,  $R - M$ , and equivalent directions) and the special points:  $\Gamma = (0, 0, 0)$ ,  $X = (\pi, 0, 0)$ ,  $M = (\pi, \pi, 0)$ ,  $R = (\pi, \pi, \pi)$ ,  $Z = (0, 0, \pi)$ .

— they are given by  $-\varepsilon_{\mathbf{k}}^{\pm}$  and separated from the lower bands (5) by a large gap of  $2J_H S$  at  $\gamma_{\mathbf{k}}^{\pm} = 0$ .

In the undoped  $G$ -AF phase of  $\text{SrMnO}_3$  spin canting is absent ( $\theta = 0$ ) and the electronic structure consists of four Slater bands  $\pm\varepsilon_{\mathbf{k}}^{\pm}$ , see Fig. 1. Both  $e_g$  orbitals are equivalent here and equally contribute to each electronic band. The lowest energy is obtained along the  $\Gamma - X$  and equivalent directions in the Brillouin zone and here electrons are doped. By considering the electron energy close to these lines one finds that the Fermi surface in the regime of low electron doping, shown in the inset in Fig. 1, consists of narrow cylinders along equivalent main directions in the reciprocal space.

The canting angle in the  $G$ -AF phase is given by

$$\sin \theta \simeq \frac{tJ_H S}{\sqrt{(3t)^2 + (J_H S)^2}} \frac{x}{12JS^2}, \quad (7)$$

and increases linearly with  $x$  in the low doping regime. Using an empirical formula for the Néel temperature of a Heisenberg antiferromagnet,<sup>26</sup> we obtained  $J = 3.79$  meV for  $\text{SrMnO}_3$  from the experimental  $T_N \simeq 230$  K.<sup>22</sup> For the parameters of Fig. 1, one finds from Eq. (7) that the canting angle is rather small,  $\sin \theta \simeq 2.7x$ , and quite close to the experimental value,  $\theta_{\text{exp}} \simeq 2x$ .<sup>22</sup>

The electronic structure  $\{\varepsilon_{\mathbf{k}}\}$  for the  $C$ -AF phase is quite distinct from the one in the  $G$ -AF phase and was determined numerically. It depends on doping  $x$  as the tetragonal lattice distortion increases with it. We have verified that this dependence is weak for the realistic parameters, i.e., with  $g \simeq 3.0$  eV and  $K \simeq 20$  eV.<sup>23</sup> A representative result is shown in Fig. 2 for  $x = 0.05$ . As the FM order along the  $c$  axis breaks the cubic symmetry, the orbitals decouple from each other in the electronic structure and form two independent subsets of bands. This is best visible along the  $\Gamma - Z$  directions where one band

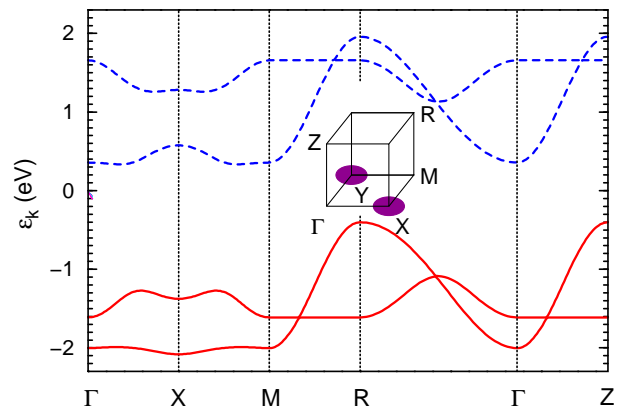


FIG. 2: (Color online) Band structure in the  $C$ -AF phase along the high symmetry directions. Spin majority (minority) bands are shown by solid (dashed) lines. Parameters:  $t = 0.4$  eV,  $J_H = 0.74$  eV,  $g = 3$  eV,  $x = 0.05$ . The special points as in Fig. 1. Inset shows the Fermi surface pockets at low doping near the  $X$  and  $Y$  points.

has a large dispersion close to  $4t$ , and the other one is dispersionless (Fig. 2). In addition, the former band has also a very weak dispersion along two (equivalent)  $\Gamma - X$  and  $\Gamma - Y$  directions, with two minima at the  $X$  and  $Y$  points that arise due to the weak mixing between  $z$  and  $x$  orbitals by hopping in  $ab$  planes, but this hopping is almost fully quenched due to the AF order.

Surprisingly, we found no spin canting in the  $C$ -AF phase. Here the spins form an ideal staggered AF structure in the  $ab$  planes, while they are aligned in FM chains along the  $c$  axis. The reason of this behavior is the electronic structure with the lowest energy at the  $X$  and  $Y$  points and the Fermi surface consisting of two pockets that are centered around these two equivalent points at low doping, see the inset in Fig. 2. For this Fermi surface topology no kinetic energy can be gained by spin canting, since the resulting nearest-neighbor hopping between  $z$  orbitals in  $ab$  planes,  $\frac{1}{4}t \sin \theta (\cos k_x + \cos k_y)$ , vanishes at the  $X$  and  $Y$  points. Thus, the observed suppression of spin canting in the  $C$ -AF phase follows from the abrupt change of the Fermi surface topology at the magnetic transition.

The consequences of flavor separated band structure in the  $C$ -AF phase are remarkable. First of all, electrons doped in  $\text{SrMnO}_3$  have pure  $z$  orbital character. Second, this implies that they can propagate only along the  $c$  axis where localized spins are FM, but their motion is blocked in the  $ab$  planes by the AF order, in agreement with DE. Altogether this leads to a dimensional reduction of electronic transport to 1D chains along the  $c$  axis.

A qualitatively different character of the electronic structure in both AF phases is visible in the orbital-resolved density of states (DOS)  $N_z(\omega)$  and  $N_x(\omega)$  in the spin majority bands, see Fig. 3. In the  $G$ -AF phase both orbital DOSs are the same and have low bandwidth of  $\sim 0.5$  eV due to the AF order in all three cubic directions [Fig. 3(a)]. At the lower band edge one finds a character-

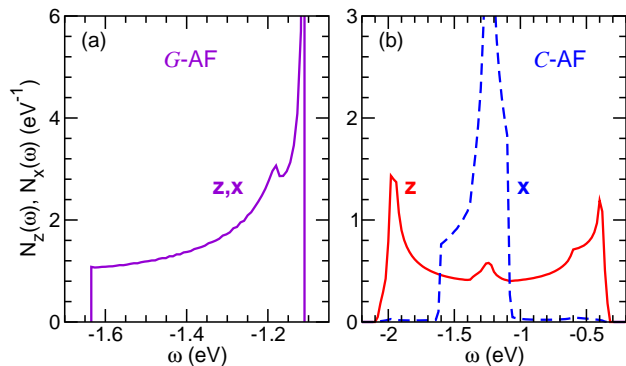


FIG. 3: (Color online) Densities of states for  $e_g$  electrons,  $N_z(\omega)$  and  $N_x(\omega)$ , in the spin majority bands as obtained for: (a) the  $G$ -AF phase ( $N_z(\omega)$  and  $N_x(\omega)$  are here degenerate) with a singularity arising from the AF order at  $\omega = -1.11$  eV, and (b) the  $C$ -AF phase; here the density of  $z$ ,  $N_z(\omega)$ , and  $x$ ,  $N_x(\omega)$ , electron states is shown by solid (red) and dashed (blue) line. Parameters:  $t = 0.4$  eV,  $J_H = 0.74$  eV; for  $C$ -AF phase in addition  $g = 3$  eV and  $x = 0.05$ .

istic step which reflects the quasi-two-dimensional DOS of  $e_g$  electrons.<sup>27</sup> A large gap between the spin majority and spin minority states in the AF phase generates a van Hove singularity at the upper edge of the DOSs.

From the DOS in the  $G$ -AF phase, see Fig. 3(a), we have estimated the coefficient  $\gamma \simeq 5$  mJ/mol·K<sup>2</sup> in the specific heat  $c_V \simeq \gamma T$  at  $x = 0.01$  which is indeed very close to the experimental value  $\gamma_{\text{exp}} \simeq 5.4$  mJ/mol·K<sup>2</sup>, and weakly increases with doping  $x$  as in experiment.<sup>22</sup> Thus we find that almost no polaronic renormalization of the electron mass occurs in  $\text{Sr}_{1-x/2}\text{Ce}_{x/2}\text{MnO}_3$  and  $\text{Sr}_{1-x}\text{La}_x\text{MnO}_3$ .

Unlike in the  $G$ -AF phase, the orbital flavors separate in the  $C$ -AF phase into a wide quasi-1D  $z$ -subband of width  $\sim 4t$  and a narrow (empty)  $x$ -subband, similar to the majority spin bands in the  $G$ -AF phase. The former subband gives a characteristic 1D DOS  $N_z(\omega)$ , with two maxima at both band edges. Due to the AF order in the  $ab$  plane, the separation of the  $e_g$  orbital flavors is almost perfect here. Large DOS  $N_z(\omega)$  at the edge of the quasi-1D band [Fig. 3(b)] is here sufficient for self-trapping of electrons<sup>28</sup> within spin polarons, as is doped  $\text{CaMnO}_3$ .<sup>29</sup> In the present case we believe that the polarons are quasi-1D, in agreement with the nature of underlying  $C$ -type structure and showing a similar behavior to orbital polarons in a 1D model of hole-doped manganites.<sup>24</sup> We thus expect a strongly anisotropic optical conductivity in the insulating  $C$ -AF phase:  $\sigma_{ab}(\omega)$  with a large gap, and a pseudometallic  $\sigma_c(\omega)$  with small charge gap.

#### IV. MAGNETIC PHASE TRANSITION

Now we show that the DE triggers the magnetic transition in an electron doped system by comparing the total energies in both magnetic phases. In the undoped sys-

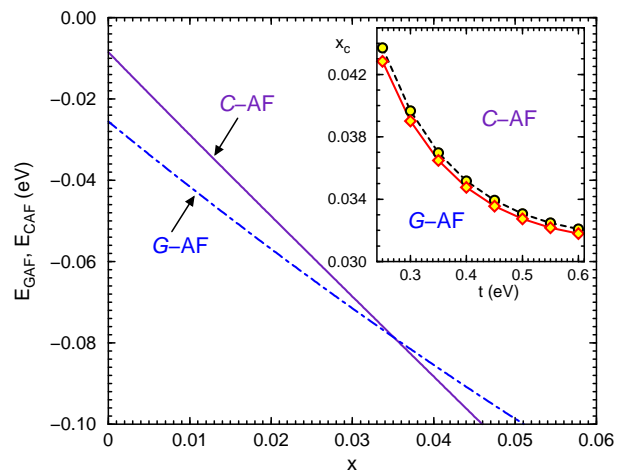


FIG. 4: (Color online) Total energies of the  $G$ -AF ( $E_{GAF}$ ) and  $C$ -AF ( $E_{CAAF}$ ) phase as obtained for increasing electron doping  $x$ . Parameters:  $t = 0.4$  eV,  $J_H = 0.74$  eV,  $g = 3$  eV,  $K = 20$  eV, and  $J = 3.79$  meV. Inset shows the phase diagram in the  $(t, x_c)$  plane obtained for:  $g = 0$  (circles, dashed line), and  $g = 3$  eV (diamonds, solid line).

tem ( $x = 0$ ) the ground state is the  $G$ -AF structure, with low magnetic energy of  $E_{GAF}^0 = -3JS^2$  per site, and this energy increases to  $-3JS^2 \cos 2\theta$  for finite doping  $x > 0$ . In the collinear  $C$ -AF phase this energy is enhanced to  $E_{CAAF}^0 = -JS^2$ , as the superexchange bonds along the  $c$  axis are here frustrated. Simultaneously, however, increasing doping gives a different kinetic energy in the above phases, obtained by summing up the energies of occupied states for a given doping  $x$ . The lower edge of the DOS is much lower in case of the  $C$ -AF phase than for the  $G$ -AF phase; for instance at  $x = 0.05$  these minima are at  $\omega_G \simeq -1.63$  eV and  $\omega_C \simeq -2.07$  eV, see Fig. 3. One finds the energy gain due to full electron hopping  $\sim t$  along the  $c$  axis in the 1D electronic structure of the  $C$ -AF phase, while only a small fraction of  $t$  contributes to the kinetic energy in the isotropic 3D  $G$ -AF phase. Therefore, the total energy of the  $C$ -AF phase decreases faster with increasing doping  $x$ , see Fig. 4, and finally this phase becomes more stable than the  $G$ -AF one for  $x > x_c$ , as observed in the experiment.<sup>22</sup> We note that small spin canting in the  $G$ -AF phase has almost no effect on the phase boundary as the gain in the kinetic energy is almost cancelled by the loss of the superexchange energy.

The crucial role played by the DE mechanism is visible in the phase diagram of electron doped manganites shown in the inset of Fig. 4. For increasing hopping  $t$  both phases have increased kinetic energy gains, but a larger energy gain is found in the  $C$ -AF phase. As a result, the critical concentration  $x_c$  is lowered when  $t$  increases, but one finds that  $x_c$  lies still in a relatively narrow window of doping  $0.03 < x_c < 0.04$  in a broad range of realistic values of  $t \in (0.3, 0.6)$  eV.

The magnetic transition is first order and occurs at a somewhat lower doping  $x_c$  when the tetragonal distortion

which stabilizes the  $C$ -AF phase is considered, see the inset of Fig. 4. However, this energy gain is rather small compared with the kinetic energy difference between the two magnetic phases, so we conclude that the tetragonal distortion has only a weak stabilizing effect for the 1D  $3z^2 - r^2$  structure in the  $C$ -AF phase, while the transition itself follows from the DE interaction. We remark that this scenario does not apply to  $\text{La}_x\text{Ca}_{1-x}\text{MnO}_3$  nanoparticles where phase separation into AF and FM domains takes place.<sup>30</sup>

## V. SUMMARY

Summarizing, we have introduced the microscopic model that explains the mechanism of the magnetic transition in electron doped manganites from canted  $G$ -AF to collinear  $C$ -AF phase at low doping  $x \simeq 0.04$ . We demonstrated that the DE supported by the cooperative Jahn-Teller effect leads then to dimensional reduction

from an isotropic 3D  $G$ -AF phase to a quasi-1D order of partly occupied  $3z^2 - r^2$  orbitals in the  $C$ -AF phase. This prediction of the theory can be verified by future angle resolved photoemission experiments as the shape of the Fermi surface in the  $G$ -AF and  $C$ -AF phases is radically different.

The presented theory explains as well the absence of spin canting in the  $C$ -AF phase by the Fermi surface topology. This is a subtle effect as electron doping occurs here near the  $X$  and  $Y$  points in the Brillouin zone, and the kinetic energy cannot be gained in spin canted structure.

## Acknowledgments

We thank Lou-Fe' Feiner and Peter Horsch for insightful discussions. A.M.O. acknowledges support by the Foundation for Polish Science (FNP) and by the Polish Ministry of Science under Project N202 069639.

- 
- <sup>1</sup> P. A. Lee, N. Nagaosa, and X.-G. Wen, *Rev. Mod. Phys.* **78**, 17 (2006); M. Vojta, *Adv. Phys.* **58**, 699 (2009).
- <sup>2</sup> J. Paglione and R. L. Greene, *Nat. Phys.* **6**, 645 (2010).
- <sup>3</sup> E. Dagotto, T. Hotta, and A. Moreo, *Phys. Rep.* **344**, 1 (2001); E. Dagotto, *New J. Phys.* **7**, 67 (2005).
- <sup>4</sup> Y. Tokura, *Rep. Prog. Phys.* **69**, 797 (2006).
- <sup>5</sup> A. Weiße and H. Fehske, *New J. Phys.* **6**, 158 (2004).
- <sup>6</sup> C. Zener, *Phys. Rev.* **82**, 403 (1951).
- <sup>7</sup> P. G. de Gennes, *Phys. Rev.* **118**, 141 (1960).
- <sup>8</sup> R. Maezono, S. Ishihara, and N. Nagaosa, *Phys. Rev. B* **58**, 11583 (1998).
- <sup>9</sup> T. Hotta, A. L. Malvezzi, and E. Dagotto, *Phys. Rev. B* **62**, 9432 (2000); A. M. Oleś and L. F. Feiner, *ibid.* **65**, 052414 (2002); D. V. Efremov, J. van den Brink, and D. I. Khomskii, *Nature Mat.* **3**, 853 (2004).
- <sup>10</sup> S. Dong, R. Yu, J.-M. Liu, and E. Dagotto, *Phys. Rev. Lett.* **103**, 107204 (2009).
- <sup>11</sup> S. Liang, M. Daghofer, S. Dong, C. Şen, and E. Dagotto, *Phys. Rev. B* **84**, 024408 (2011).
- <sup>12</sup> G. Jackeli and G. Khaliullin, *Phys. Rev. Lett.* **101**, 216804 (2008).
- <sup>13</sup> R. J. McQueeney, M. Yethiraj, S. Chang, W. Montfrooij, T. G. Perring, J. M. Honig, and P. Metcalf, *Phys. Rev. Lett.* **99**, 246401 (2007); **100**, 069901(E) (2008).
- <sup>14</sup> Y. Motome and N. Furukawa, *Phys. Rev. Lett.* **104**, 106407 (2010); S. Kumar and J. van den Brink, *ibid.* **105**, 216405 (2010).
- <sup>15</sup> G.-W. Chern and C. D. Batista, *Phys. Rev. Lett.* **107**, 186403 (2011).
- <sup>16</sup> In the  $C$ -AF ( $A$ -AF) phase the spin order parameter is staggered in  $ab$  planes (along the  $c$  axis), while in the  $G$ -AF phase it is staggered in all three cubic directions.
- <sup>17</sup> J. van den Brink and D. Khomskii, *Phys. Rev. Lett.* **82**, 1016 (1999).
- <sup>18</sup> I. Leonov, D. Korotin, N. Binggeli, V. I. Anisimov, and D. Vollhardt, *Phys. Rev. B* **81**, 075109 (2010).
- <sup>19</sup> L. F. Feiner and A. M. Oleś, *Phys. Rev. B* **59**, 3295 (1999).
- <sup>20</sup> Z. Zeng, M. Greenblatt, and M. Croft, *Phys. Rev. B* **63**, 224410 (2001); E. N. Caspi, M. Avdeev, S. Short, J. D. Jorgensen, M. V. Lobanov, Z. Zeng, M. Greenblatt, P. Thiyagarajan, C. E. Botez, and P. W. Stephens, *ibid.* **69**, 104402 (2004).
- <sup>21</sup> H. Tsukahara, S. Ishibashi, and K. Terakura, *Phys. Rev. B* **81**, 214108 (2010).
- <sup>22</sup> H. Sakai, S. Ishiwata, D. Okuyama, A. Nakao, H. Nakao, Y. Murakami, Y. Taguchi, and Y. Tokura, *Phys. Rev. B* **82**, 180409 (2010).
- <sup>23</sup> R. Kilian and G. Khaliullin, *Phys. Rev. B* **60**, 13458 (1999).
- <sup>24</sup> M. Daghofer, A. M. Oleś, and W. von der Linden, *Phys. Rev. B* **70**, 184430 (2004).
- <sup>25</sup> A. M. Oleś, P. Horsch, G. Khaliullin, and L. F. Feiner, *Phys. Rev. B* **72**, 214431 (2005); N. N. Kovaleva, A. M. Oleś, A. M. Balbashov, A. Maljuk, D. N. Argyriou, G. Khaliullin, and B. Keimer, *ibid.* **81**, 235130 (2010).
- <sup>26</sup> G. S. Rushbrooke and P. J. Wood, *Mol. Phys.* **1**, 257 (1958); M. Fleck, M. G. Zacher, A. I. Lichtenstein, W. Hanke, and A. M. Oleś, *Eur. Phys. J. B* **37**, 439 (2004).
- <sup>27</sup> L. F. Feiner and A. M. Oleś, *Phys. Rev. B* **71**, 144422 (2005).
- <sup>28</sup> G. Wellein and H. Fehske, *Phys. Rev. B* **58**, 6208 (1998).
- <sup>29</sup> H. Meskine, T. Saha-Dasgupta, and S. Satpathy, *Phys. Rev. Lett.* **92**, 056401 (2004).
- <sup>30</sup> Y. Wang and H. J. Fan, *Phys. Rev. B* **83**, 224409 (2011).